2011

Patterns of morphological variation amongst semifossorial shrews in the highlands of Guatemala, with the description of a new species (Mammalia, Soricomorpha, Soricidae)

Neal Woodman
USGS Patuxent Wildlife Research Center, woodmann@si.edu

The LINNEAN SOCIETY of London ZOOLOGICAL Journal of the Linnean Society

Zoological Journal of the Linnean Society, 2011, **163**, 1267–1288. With 10 figures

Patterns of morphological variation amongst semifossorial shrews in the highlands of Guatemala, with the description of a new species (Mammalia, Soricomorpha, Soricidae)

NEAL WOODMAN*

USGS Patuxent Wildlife Research Center, National Museum of Natural History, Smithsonian Institution, Washington, DC, 20013-7012, USA

Received 26 January 2011; revised 6 April 2011; accepted for publication 14 April 2011

Members of the *Cryptotis goldmani* group of small-eared shrews (Mammalia, Soricomorpha, Soricidae) represent a clade within the genus that is characterized by modifications of the forelimb that include broadened forefeet, elongated and broadened foreclaws, and massive humeri with enlarged processes. These modifications are consistent with greater adaptation to their semifossorial habits than other members of the genus. The species in this group occur discontinuously in temperate highlands from southern Tamaulipas, Mexico, to Honduras. In Guatemala, there are three species: the relatively widespread *Cryptotis goodwini* and two species (*Cryptotis lacertosus*, *Cryptotis mam*) endemic to highland forests in the Sierra de los Cuchumatanes of western Guatemala. Ongoing studies focusing on the relationships of variation in cranial and postcranial skeletal morphology have revealed a fourth species from remnant cloud forest in the Sierra de Yalijux, central Guatemala. In this paper, I describe this new species and characterize its morphology relative to other species in the *C. goldmani* group and to other species of *Cryptotis* in Guatemala. In addition, I summarize available details of its habitat and ecology.

doi: 10.1111/j.1096-3642.2011.00754.x

ADDITIONAL KEYWORDS: Blarinini – Central America – Eulipotyphla – humerus – Insectivora – manus – Soricinae.

INTRODUCTION

The genus *Cryptotis* comprises at least 32 species (Hutterer, 2005; Woodman, 2010) of small-eared shrews that are discontinuously distributed from the eastern USA and southernmost Canada to the northern Andes of South America. These species are generally divided amongst four species groups based on a combination of external characteristics and cranial and postcranial morphology. The *Cryptotis parvus* group is distributed from north-eastern North America to central Costa Rica; the *Cryptotis nigrescens* group is known from southern Mexico to northern Colombia; the *Cryptotis thomasi* group, consisting primarily of South American species, occurs in Panama and in the Andean Cordillera from Venezuela into northern Peru; and the *Cryptotis mexicanus* group is found in highlands from Tamaulipas, Mexico, to Honduras (Choate, 1970; Woodman & Timm, 1993, 1999; Woodman & Péfaur, 2008).

Species in the *C. mexicanus* group are notable because they possess a number of modifications of the forelimb that appear to be adaptations for digging. Externally, the forefeet are wide, and the foreclaws are broad and elongate relative to those of other species in the genus. These features are accompanied in the skeleton of the manus by short and broad metacarpals, proximal phalanges, and middle phalanges, and by long broad distal phalanges (Woodman &

*E-mail: woodmann@si.edu

Timm, 1999; Woodman & Morgan, 2005; Woodman & Stephens, 2010). The humerus also is more robust in these species, and processes of the humerus, such as the medial and lateral epicondyles and teres tubercle, are greatly enlarged, resulting in larger surfaces for more extensive muscle attachment. A subset of the *C. mexicanus* group, known as the broad-clawed shrews or *Cryptotis goldmani* group, includes the largest species, and they possess the most extreme forelimb modifications (Woodman & Timm, 1999; Woodman, 2010).

Six species of small-eared shrews are currently known from Guatemala: *Cryptotis tropicalis* (Merriam, 1895) is part of the *C. parvus* group; *Cryptotis mayensis* (Merriam, 1901c) and *Cryptotis merriami* Choate, 1970 are both members of the *C. nigrescens* group; and *Cryptotis goodwini* Jackson, 1933, *Cryptotis lacertosus* Woodman, 2010, and *Cryptotis mam* Woodman, 2010 are broad-clawed shrews of the *C. goldmani* group. *Cryptotis goodwini* is relatively widespread in Guatemala, whereas *C. lacertosus* and *C. mam* are endemic to distinct portions of the Sierra de los Cuchumatanes in western Guatemala. Analyses of cranial and postcranial anatomy of populations of broad-clawed shrews in Central American and southern Mexico have revealed a fourth distinctive population from the Sierra de Yalijux in central Guatemala that is also distinguishable by its darker pelage. Herein, I describe this species and show how it differs from other members of the genus based on a combination of characteristics derived mostly from the skull and the postcranial skeleton.

MATERIAL AND METHODS

All measurements are in millimetres and all weights are in grams. Tabular univariate statistics include mean ± SD and range. Comparative terms are in reference to species in the genus *Cryptotis*, unless otherwise specified. External measurements were taken from specimen labels or field notes of the original collectors, except length of the head and body, which was determined by subtracting tail length from total length. Twenty-one skull variables, described and illustrated by Woodman & Timm (1993), were measured to the nearest 0.1 mm using a digital caliper or an ocular micrometer in a dissection microscope. Abbreviations used for external and skull measurements are provided in Table 1. Seven variables were measured on the humerus (Fig. 1), and their abbreviations are given in Table 2. X-ray images of the manus were taken from dried skins and transferred to Adobe Photoshop CS3 (version 10.0.1, San Jose, CA, USA), where they were converted to positive images, trimmed, and measured using the custom measurement scale in the Analysis menu (Woodman & Stephens, 2010). A total of 28 variables was measured on the metacarpals and phalanges of rays I, III, and V. These were rounded to the nearest 0.01 mm and are presented with their respective abbreviations in Tables 3–5. Capitalized colour terms used for the pelage are from Ridgway (1912). In accordance with Opinion 2164 of the ICZN (2006), the genus *Cryptotis* is treated as masculine.

For most analyses, I used six groupings of specimens representing the holotype of *Cryptotis goodwini magnimanus* Woodman & Timm, 1999, four recognized species of broad-clawed *Cryptotis* (*C. goodwini*, *C. griseoventris* Jackson, 1933, *C. lacertosus*, *C. mam*), and individuals of the new species labelled and referred to as 'Alta Verapaz' for the purpose of these tests. As the results of a variety of tests indicate that *C. goodwini magnimanus* differs from other *C. goodwini* in a number of morphological features, I subsequently treat this specimen as representing a distinct species, hereafter referred to as *C. magnimanus*. Specimens examined and measured for this study (see Appendix) are deposited in the following collections (abbreviations in parentheses): American Museum of Natural History, New York (AMNH); The Natural History Museum, London (BMNH); Field Museum of Natural History, Chicago (FMNH); University of Kansas Natural History Museum, Lawrence (KU); Museum of Comparative Zoology, Cambridge (MCZ); University of Michigan Museum of Zoology, Ann Arbor (UMMZ); National Museum of Natural History, Washington (USNM).

I initiated statistical analyses of skull and postcranial features to help determine whether new specimens obtained from field work in Alta Verapaz could be identified as one of the five recognized species of broad-clawed *Cryptotis* known from the region. These five species overlap to varying degrees in body size (Table 1), and they lack readily obvious characters that can be used to identify them consistently in the field. To characterize intraspecific and interspecific variation in morphology of the skulls, humeri, and forefeet, and to graphically compare the new species to other broad-clawed *Cryptotis*, I carried out principal components analyses (PCAs) on correlation matrices of ten $\log_{10}$-transformed craniomandibular variables [length of palate (PL), breadth of zygomatic plate (ZP), postorbital breadth (PO), length of maxillary toothrow (TR), length of unicuspid toothrow (UTR), breadth across second molars (M2B), height of coronoid process (HCP), length of metacarpal (ML), height of condylar valley (HCV), length of upper first molar (M1L)] using SYSTAT 11 (Cranes Software International, Bangalore, India). The largest cranial measurement (CBL) was excluded from these analyses to increase sample sizes. The first test included 25 *C. goodwini*, eight *C. griseoventris*, eight *C. lacer-*

Table 1. External and craniomandibular measurements (mm) from six species of broad-clawed *Cryptotis*

Measurements	*Cryptotis griseoventris*	*Cryptotis mam*	*Cryptotis magnimanus*	Alta Verapaz	*Cryptotis lacertosus*	*Cryptotis goodwini*
External measurements						
	(*N* = 10)	(*N* = 28)	(*N* = 1)	(*N* = 3)	(*N* = 8)	(*N* = 32)
Head and body length (HB)						
	79 ± 4	75 ± 4	80	82 ± 5	82 ± 4	84 ± 5
	73–85	64–81		77–86	75–87	75–94
Tail length (TL)						
	30 ± 2	29 ± 2	25	30 ± 2	28 ± 2	29 ± 2
	27–31	22–32		28–32	24–30	25–34
Length of hind foot (HF)						
	15 ± 1	14 ± 1	14	15	14 ± 1	15 ± 1
	14–16	11–16			12–15	14–17
						(*N* = 30)
Weight (WT)						
	–	9 ± 1	–	13 ± 3	15 ± 3	17 ± 1
		7–11		10–15	10–17	16–19
		(*N* = 9)			(*N* = 7)	(*N* = 9)
Cranial measurements						
	(*N* = 8)	(*N* = 21)	(*N* = 1)	(*N* = 5)	(*N* = 8)	(*N* = 19)
Condylobasal length (CBL)						
	19.9 ± 0.3	19.9 ± 0.4	20.3	21.4 ± 0.2	21.5 ± 0.6	21.0 ± 0.5
	19.4–20.3	18.8–20.4		21.1–21.5	20.8–22.8	20.0–21.8
				(*N* = 3)		
Breadth of braincase (BB)						
	10.2 ± 0.2	10.2 ± 0.2	10.8	10.9 ± 0.4	11.0 ± 0.3	11.2 ± 0.3
	9.8–10.5	10.0–10.7		10.5–11.3	10.8–11.6	10.8–11.6
				(*N* = 3)	(*N* = 7)	(*N* = 15)
Breadth of zygomatic plate (ZP)						
	1.9 ± 0.1	2.0 ± 0.1	2.2	2.1 ± 0.3	2.1 ± 0.2	1.9 ± 0.1
	1.8–2.1	1.6–2.1		1.6–2.7	1.8–2.5	1.6–2.2
				(*N* = 7)		
Postorbital breadth (PO)						
	5.1 ± 0.1	5.2 ± 0.2	5.3	5.5 ± 0.2	5.3 ± 0.2	5.6 ± 0.2
	4.8–5.2	4.8–5.4		5.3–5.7	5.1–5.7	5.3–5.8
				(*N* = 6)		
Breadth across first unicuspids (U1B)						
	2.4 ± 0.1	2.5 ± 0.1	2.6	2.7 ± 0.1	2.7 ± 0.1	2.7 ± 0.1
	2.3–2.6	2.4–2.6		2.5–2.8	2.6–2.9	2.6–2.9
				(*N* = 4)		
Breadth across third unicuspids (U3B)						
	3.0 ± 0.1	3.0 ± 0.1	3.0	3.2 ± 0.2	3.3 ± 0.1	3.3 ± 0.1
	2.8–3.1	2.9–3.2		3.0–3.3	3.2–3.5	3.0–3.4
				(*N* = 4)		
Breadth across second molars (M2B)						
	5.6 ± 0.1	5.7 ± 0.1	5.9	6.2 ± 0.2	5.9 ± 0.2	6.2 ± 0.2
	5.4–5.8	5.5–5.9		5.9–6.4	5.7–6.3	6.0–6.7
Length of palate (PL)						
	8.9 ± 0.2	8.7 ± 0.2	8.8	9.4 ± 0.4	9.3 ± 0.3	9.2 ± 0.2
	8.6–9.1	8.1–9.1		9.0–10.1	9.0–10.1	8.8–9.5
				(*N* = 7)		
Length of maxillary toothrow (TR)						
	7.7 ± 0.2	7.6 ± 0.2	7.5	8.3 ± 0.2	8.0 ± 0.3	7.9 ± 0.2
	7.5–8.0	7.2–8.0		8.1–8.5	7.7–8.6	7.5–8.3
Length of unicuspid toothrow (UTR)						
	2.8 ± 0.1	2.7 ± 0.1	2.4	2.9 ± 0.1	2.8 ± 0.1	2.7 ± 0.1
	2.6–2.9	2.5–2.8		2.7–2.9	2.7–2.9	2.5–2.9
Length of molariform toothrow (MTR)						
	5.3 ± 0.2	5.2 ± 0.1	5.5	5.8 ± 0.2	5.6 ± 0.2	5.6 ± 0.2
	5.0–5.5	5.0–5.5		5.5–6.0	5.4–5.8	5.3–5.9
				(*N* = 6)		
Posterior width of upper first molar (WM1)						
	1.6	1.7 ± 0.1	1.8	1.8 ± 0.1	1.7 ± 0.1	1.8 ± 0.1
	1.6–1.6	1.6–1.8		1.7–2.0	1.6–1.9	1.7–1.9
	(*N* = 5)	(*N* = 11)		(*N* = 7)		(*N* = 15)
Mandibular measurements						
	(*N* = 8)	(*N* = 21)	(*N* = 1)	(*N* = 5)	(*N* = 8)	(*N* = 19)
Length of mandible (ML)						
	6.2 ± 0.2	6.1 ± 0.2	6.5	6.8 ± 0.1	6.4 ± 0.2	6.6 ± 0.2
	5.9–6.4	5.7–6.4		6.7–6.9	6.2–6.8	6.2–7.0

Table 1. *Continued*

Measurements	*Cryptotis griseoventris*	*Cryptotis mam*	*Cryptotis magnimanus*	Alta Verapaz	*Cryptotis lacertosus*	*Cryptotis goodwini*
Height of coronoid process (HCP)						
	4.3 ± 0.05	4.4 ± 0.1	4.7	4.7 ± 0.1	4.6 ± 0.1	4.8 ± 0.1
	4.3–4.4	4.2–4.8		4.6–4.9	4.5–4.8	4.6–5.2
Height of condylar valley (HCV)						
	2.8 ± 0.1	2.8 ± 0.1	2.9	3.0 ± 0.1	2.9 ± 0.1	3.0 ± 0.1
	2.6–2.8	2.6–3.0		2.9–3.2	2.8–3.1	2.8–3.4
Height of articular process (HAC)						
	3.8 ± 0.1	3.9 ± 0.1	4.1	4.1 ± 0.2	4.1 ± 0.2	4.2 ± 0.2
	3.7–3.9	3.7–4.1		3.9–4.2 ($N = 4$)	3.9–4.5	3.8–4.6
Articular process to lower third molar (AC3)						
	5.1 ± 0.1	5.1 ± 0.1	5.3	5.5 ± 0.3	5.4 ± 0.3	5.6 ± 0.2
	4.9–5.3	4.8–5.3		5.1–5.8 ($N = 4$)	5.1–5.8	5.2–5.9
Breadth of articular condyle (BAC)						
	3.0 ± 0.1	3.0 ± 0.1	3.1	3.3 ± 0.2	3.3 ± 0.1	3.3 ± 0.2
	2.9–3.1	2.8–3.2		3.0–3.3 ($N = 4$)	3.2–3.6	3.0–3.6
Length of mandibular toothrow (TRM)						
	6.1 ± 0.2	6.1 ± 0.2	5.9	6.5 ± 0.2	6.4 ± 0.2	6.4 ± 0.2
	5.8–6.4	5.8–6.3		6.3–6.7	6.2–6.8	6.1–6.7
Length mandibular molar row (m13)						
	4.3 ± 0.1	4.3 ± 0.1	4.4	4.7 ± 0.2	4.6 ± 0.1	4.7 ± 0.1
	4.1–4.6	4.1–4.5		4.6–5.0	4.5–4.9	4.4–4.9
Length of lower first molar (m1L)						
	1.8 ± 0.1	1.7 ± 0.1	1.8	1.8 ± 0.1	1.9 ± 0.1	1.9 ± 0.1
	1.7–1.9	1.6–1.8		1.8–1.9	1.8–2.0	1.8–2.0

Species are ordered by condylobasal length.
Statistics are mean ± SD and range.

tosus, the holotype of *C. magnimanus*, 26 *C. mam*, and four individuals of the new species. As the new species proved closest in multivariate space to the two largest species, I restricted a second set of analyses to *C. goodwini*, *C. lacertosus*, and the new species. To compare humeri, I used seven variables [breadth of shaft (BS1), distance from deltoid process to capitulum (CD), width of distal end of humerus (DW), distance from greater tuberosity to teres tubercle (GT), length of humerus from head to capitulum and trochlea (L1), internal distance from medial epicondyle to teres tubercle (MT), proximal width (PW)] measured from two *C. goodwini*, four *C. lacertosus*, one *C. magnimanus*, nine *C. mam*, and three individuals of the new species. The humerus of *C. griseoventris* is unknown. In comparing forefeet, I used six variables [1ML, width of metacarpal (1MW), length of proximal phalanx (1PPL), width of proximal phalanx (1PPW), length of distal phalanx (1DPL), width of distal phalanx (1DPW)] from ray I, measured from 16 *C. goodwini*, four *C. griseoventris*, six *C. lacertosus*, 25 *C. mam*, and two individuals of the new species; eight variables [3ML, 3MW, 3PPL, 3PPW, length of middle phalanx (3MPL), width of middle phalanx (3MPW), 3DPL, 3DPW] from ray III, measured from 14 *C. goodwini*, eight *C. griseoventris*, five *C. lacertosus*, 22 *C. mam*, and two individuals of the new species; and six variables (5PPL, 5PPW, 5MPL, 5MPW, 5DPL, 5DPW) from ray V, measured from 15 *C. goodwini*, seven *C. griseoventris*, six *C. lacertosus*, 18 *C. mam*, and two individuals of the new species. In the last test, the measurements 5ML and 5MW were excluded to increase sample sizes. The manus skeleton of *C. magnimanus* is unknown.

To examine overall similarity in morphology amongst the six species of large-footed *Cryptotis* from the region, I used hierarchical cluster analyses on variable means, both for individual elements (i.e. skull, humerus, and individual rays) and for all data combined. These analyses were based on 21 craniomandibular variables; seven humerus variables; eight variables for ray I; and ten variables each for ray III and ray V. The combined analysis included these 56 variables and three external variables (HB, TL, length of hind foot).

RESULTS

SKULL VARIABLES

The skulls of the six broad-clawed *Cryptotis* are grossly similar in overall aspect and in most qualitative characters, differing primarily in size and proportions. In a plot of factor scores from the first PCA

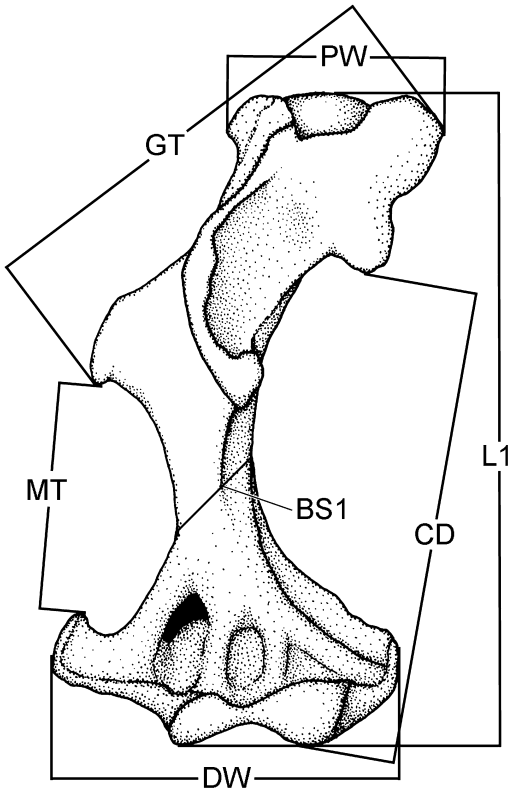

Figure 1. Anterior aspect of the humerus illustrating variables measured: BS1, breadth of shaft of humerus from superior base of medial epicondyle to superior base of lateral epicondyle; CD, distance from deltoid process to capitulum; DW, width of distal end of humerus; GT, distance from greater tuberosity to teres tubercle; L1, length of humerus from head to capitulum and trochlea; MT, internal distance from medial epicondyle to teres tubercle; PW, width of proximal end of humerus.

of skull variables from all six species, the first factor axis (representing overall quantitative size, but with little contribution from the variables UTR, ZP – Fig. 2, Table 6), separates the species into two primary subsets: smaller species, including *C. griseoventris*, *C. mam*, and *C. magnimanus*, and larger species, represented by *C. goodwini* and the Alta Verapaz sample. Most individuals of *C. lacertosus* fall between the two subsets, overlapping with both smaller and larger species, although my sample of this species includes the largest individual in the analysis. This individual (UMMZ 117843) is the younger (based on toothwear) of two *C. lacertosus* from Yayquich. The second specimen (USNM 569368) from Yayquich is an old adult, and it plots near the centre of the distribution for the species (x coordinate = 0.0836). The larger individual, although probably atypical, provides a measure of the extent of potential size variation in this species. The second factor axis principally represents UTR (Table 6). Within the subset of smaller species, *C. griseoventris* averages a longer unicuspid toothrow than *C. mam*, whereas *C. magnimanus* is distinguished by its short unicuspid toothrow. The holotype of *C. magnimanus* has moderately worn dentition, but it is unlikely that the short UTR is entirely attributable to wear. Other dental variables (TR, MTR) measured from this specimen are also short relative to condylobasal length (Table 1), and small dentition appears to characterize this species. Amongst the subset of larger species, the Alta Verapaz sample averages a longer UTR than *C. goodwini*, whereas individuals of *C. lacertosus* overlap with both *C. goodwini* and the Alta Verapaz sample. The second factor axis also separates the Alta Verapaz sample from *C. magnimanus* and *C. mam*.

In the plot of factor scores from the PCA of skull variables representing the three largest species, factor 1 (size, but with little to no contribution from half of the variables – Table 7, Fig. 3) does not distinguish the three taxa. Specimens in the Alta Verapaz sample are larger than most individuals of *C. lacertosus* with the exception of the large individual from Yayquich (UMMZ 117843), which indicates the potential for overlap in size between these two groups. Factor 2 in this analysis represents a combination of three negatively weighted variables (UTR, TR, PL) that all relate to the length of the maxillary area of the cranium. Along this axis, the Alta Verapaz sample and *C. lacertosus* separate from *C. goodwini*, reflecting their longer palates and unicuspid and maxillary toothrows (Table 7).

In summary, statistical analyses of the skulls separate the Alta Verapaz sample from *C. griseoventris*, *C. magnimanus*, and *C. mam* based on its larger skull size, and from *C. goodwini*, *C. magnimanus*, and *C. mam* based on its longer unicuspid toothrow, maxillary toothrow, and palate. The Alta Verapaz sample cannot be unequivocally separated from *C. lacertosus* on the basis of these skull measurements alone.

Humerus variables

In contrast to the skulls, the humeri of some broad-clawed shrews exhibit distinct qualitative characters that are useful in distinguishing amongst species. In a plot of PCA factor scores using seven variables from the humerus, the majority of the interspecific separation is provided by the factor 1 axis, which represents size (but with a negative contribution by MT – Table 8, Fig. 4). The humeri fall into three size classes along this axis: a subset representing the smallest humeri consists primarily of *C. mam*, but includes one specimen from the Alta Verapaz sample; a subset representing intermediate-sized humeri includes the

Table 2. Measurements of the humerus from five species of broad-clawed *Cryptotis*

Measurements	*Cryptotis mam* (*N* = 9)	Alta Verapaz (*N* = 3)	*Cryptotis goodwini* (*N* = 2)	*Cryptotis magnimanus* (*N* = 1)	*Cryptotis lacertosus* (*N* = 3)
Length (L1)					
	7.6 ± 0.2	8.0 ± 0.3	8.1, 8.3	8.2	8.7 ± 0.3
	7.4–7.8	7.7–8.2			8.4–8.9
Proximal width (PW)					
	2.5 ± 0.1	2.7 ± 0.1	2.7, 2.8	2.8	3.2 ± 0.1
	2.4–2.7	2.6–2.8			3.2–3.3
Distal width (DW)					
	4.1 ± 0.1	4.5 ± 0.2	4.5, 4.7	4.5	5.3 ± 0.2
	4.0–4.2	4.3–4.6			5.1–5.4
Greater tuberosity to teres tubercle (GT)					
	5.0 ± 0.2	5.5 ± 0.4	5.3, 5.3	5.3	5.9 ± 0.2
	4.7–5.2	5.0–5.8			5.6–6.0
Medial epicondyle to teres tubercle (MT)					
	2.6 ± 0.2	2.6 ± 0.1	2.7, 2.8	2.8	2.3 ± 0.2
	2.4–3.0	2.5–2.7			2.2–2.5
Deltoid process to capitulum (CD)					
	5.7 ± 0.2	5.8 ± 0.2	5.6, 6.2	6.0	6.1 ± 0.1
	5.4–5.9	5.7–6.0			6.0–6.2
Breadth of shaft (BS1)					
	1.0 ± 0.1	1.1 ± 0.1	1.1, 1.1	1.1	1.3 ± 0.1
	0.9–1.1	1.0–1.2			1.3–1.4

Species are ordered by humerus length.
Statistics are mean ± SD and range.

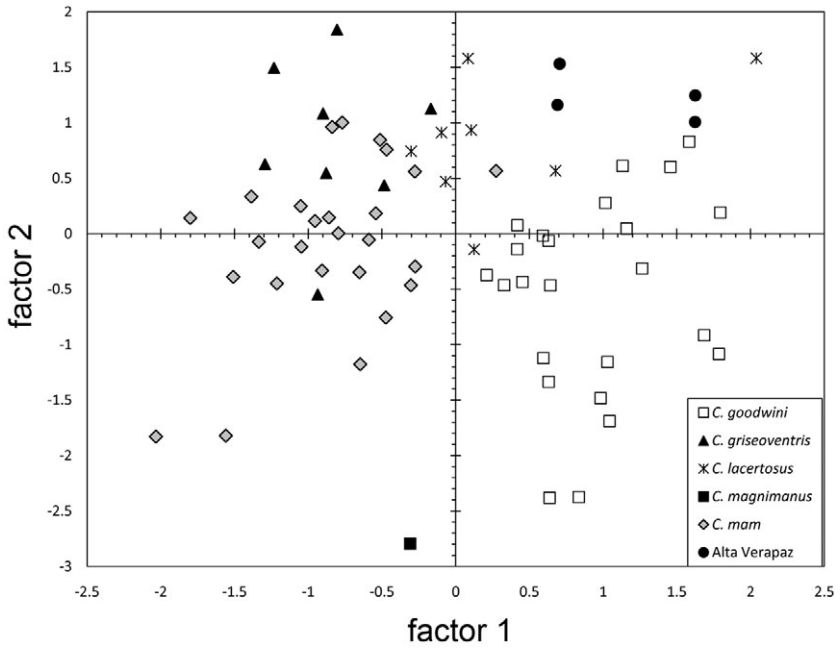

Figure 2. Plot of scores on first two axes from principal components analysis of skulls of six species of broad-clawed *Cryptotis* (see Table 6).

Table 3. Measurements (mm) of bones and claws from ray I of the manus from five species of broad-clawed *Cryptotis*

Measurements	*Cryptotis griseoventris* (*N* = 8)	*Cryptotis mam* (*N* = 26)	Alta Verapaz (*N* = 3)	*Cryptotis goodwini* (*N* = 16)	*Cryptotis lacertosus* (*N* = 6)
Length of metacarpal (1ML)					
	1.20 ± 0.05	1.21 ± 0.07	1.32, 1.40	1.35 ± 0.08	1.13 ± 0.07
	1.12–1.27	1.08–1.33	(*N* = 2)	1.22–1.47	1.06–1.22
		(*N* = 26)			
Width of metacarpal (1MW)					
	0.34 ± 0.03	0.38 ± 0.03	0.35, 0.45	0.49 ± 0.04	0.53 ± 0.05
	0.29–0.37	0.33–0.47	(*N* = 2)	0.40–0.55	0.47–0.61
		(*N* = 25)		(*N* = 15)	
Length of proximal phalanx (1PPL)					
	1.18 ± 0.09	1.15 ± 0.08	1.29 ± 0.04	1.23 ± 0.12	1.22 ± 0.09
	1.01–1.28	0.96–1.34	1.24–1.33	1.01–1.50	1.11–1.40
Width of proximal phalanx (1PPW)					
	0.33 ± 0.04	0.34 ± 0.02	0.39, 0.40	0.43 ± 0.02	0.60 ± 0.03
	0.30–0.38	0.29–0.38	(*N* = 2)	0.39–0.48	0.56–0.63
	(*N* = 4)	(*N* = 25)		(*N* = 15)	
Length of distal phalanx (1DPL)					
	1.05 ± 0.05	1.13 ± 0.05	1.28 ± 0.12	1.21 ± 0.09	1.19 ± 0.08
	0.96–1.13	0.97–1.24	1.14–1.35	1.00–1.35	1.10–1.28
Width of distal phalanx (1DPW)					
	0.46 ± 0.02	0.50 ± 0.04	0.54, 0.55	0.61 ± 0.03	0.60 ± 0.03
	0.42–0.49	0.43–0.58	(*N* = 2)	0.55–0.67	0.56–0.63
		(*N* = 25)		(*N* = 15)	
Length of claw (1CL)					
	1.91 ± 0.11	1.98 ± 0.09	2.35 ± 0.16	1.83 ± 0.17	1.79 ± 0.17
	1.77–2.10	1.77–2.14	2.26–2.54	1.37–2.08	1.58–2.00
		(*N* = 24)			
Width of claw (1CW)					
	0.26 ± 0.02	0.28 ± 0.02	0.40	0.36 ± 0.05	0.32 ± 0.05
	0.25–0.28	0.23–0.32	(*N* = 1)	0.29–0.46	0.27–0.38
	(*N* = 3)	(*N* = 14)		(*N* = 11)	(*N* = 5)

Species are ordered by width of metacarpal. Statistics are mean ± SD and range.
Variations in sample sizes appear in parentheses.

Table 4. Measurements (mm) of bones and claws from ray III of the manus from five species of broad-clawed *Cryptotis*

	Cryptotis griseoventris (*N* = 8)	*Cryptotis mam* (*N* = 26)	Alta Verapaz (*N* = 3)	*Cryptotis goodwini* (*N* = 16)	*Cryptotis lacertosus* (*N* = 6)
Length of metacarpal (3ML)					
	2.59 ± 0.07	2.59 ± 0.09	2.84 ± 0.13	2.65 ± 0.10	2.64 ± 0.10
	2.50–2.73	2.46–2.80	2.72–2.98	2.49–2.84	2.48–2.80
Width of metacarpal (3MW)					
	0.40 ± 0.02	0.45 ± 0.02	0.47 ± 0.05	0.54 ± 0.02	0.55 ± 0.01
	0.37–0.43	0.40–0.50	0.42–0.52	0.49–0.58	0.53–0.56
		(*N* = 22)			(*N* = 5)
Length of proximal phalanx (3PPL)					
	1.46 ± 0.06	1.53 ± 0.08	1.67 ± 0.10	1.60 ± 0.09	1.55 ± 0.08
	1.38–1.52	1.41–1.72	1.56–1.75	1.41–1.82	1.43–1.65
Width of proximal phalanx (3PPW)					
	0.41 ± 0.02	0.46 ± 0.03	0.53 ± 0.05	0.56 ± 0.02	0.57 ± 0.02
	0.38–0.44	0.41–0.53	0.48–0.57	0.53–0.60	0.54–0.60
		(*N* = 27)		(*N* = 14)	
Length of middle phalanx (3MPL)					
	0.90 ± 0.05	0.92 ± 0.08	0.93 ± 0.02	1.03 ± 0.10	1.03 ± 0.10
	0.82–0.96	0.77–1.06	0.92–0.95	0.89–1.16	0.87–1.18
Width of middle phalanx (3MPW)					
	0.41 ± 0.03	0.45 ± 0.03	0.53 ± 0.05	0.55 ± 0.03	0.53 ± 0.02
	0.38–0.46	0.39–0.49	0.48–0.58	0.52–0.62	0.51–0.55
				(*N* = 14)	
Length of distal phalanx (3DPL)					
	1.52 ± 0.06	1.80 ± 0.07	1.94 ± 0.16	2.03 ± 0.08	1.92 ± 0.09
	1.44–1.61	1.68–1.97	1.76–2.07	1.90–2.18	1.79–2.04
		(*N* = 27)			
Width of distal phalanx (3DPW)					
	0.56 ± 0.02	0.63 ± 0.04	0.68 ± 0.05	0.75 ± 0.04	0.72 ± 0.02
	0.53–0.59	0.56–0.71	0.63–0.72	0.65–0.80	0.69–0.75
				(*N* = 13)	
Length of claw (3CL)					
	2.79 ± 0.22	3.20 ± 0.13	3.49 ± 0.39	3.41 ± 0.20	3.28 ± 0.27
	2.34–3.08	2.92–3.43	3.14–3.91	3.11–3.76	2.94–3.66
		(*N* = 27)			
Width of claw (3CW)					
	0.42 ± 0.03	0.46 ± 0.03	0.56, 0.57	0.57 ± 0.05	0.53 ± 0.02
	0.39–0.45	0.42–0.51	(*N* = 2)	0.49–0.67	0.50–0.56
	(*N* = 4)	(*N* = 8)		(*N* = 12)	(*N* = 5)

Species are ordered by width of metacarpal.
Statistics are mean ± SD and range.
Variations in sample sizes appear in parentheses.

Table 5. Measurements (mm) of bones and claws from ray V of the manus from five species of broad-clawed *Cryptotis*

Measurements	*Cryptotis griseoventris* (*N* = 7)	*Cryptotis mam* (*N* = 24)	Alta Verapaz (*N* = 3)	*Cryptotis lacertosus* (*N* = 6)	*Cryptotis goodwini* (*N* = 15)
Length of metacarpal (ML)					
	1.68 ± 0.07	1.67 ± 0.08	1.69, 1.77	1.78 ± 0.11	1.79 ± 0.09
	1.58–1.76	1.50–1.84	(*N* = 2)	1.61–1.90	1.64–1.94
Width of metacarpal (MW)					
	0.39 ± 0.04	0.41 ± 0.03	0.46, 0.51	0.51 ± 0.04	0.55 ± 0.03
	0.34–0.43	0.37–0.48	(*N* = 2)	0.46–0.57	0.50–0.62
		(*N* = 21)			
Length of proximal phalanx (PPL)					
	1.13 ± 0.03	1.17 ± 0.10	1.20, 1.27	1.22 ± 0.04	1.26 ± 0.06
	1.08–1.17	0.87–1.41	(*N* = 2)	1.17–1.26	1.14–1.41
Width of proximal phalanx (PPW)					
	0.33 ± 0.03	0.36 ± 0.03	0.40 ± 0.02	0.43 ± 0.02	0.44 ± 0.03
	0.28–0.36	0.30–0.44	0.38–0.42	0.39–0.44	0.40–0.49
Length of middle phalanx (MPL)					
	0.76 ± 0.03	0.76 ± 0.08	0.85, 0.89	0.78 ± 0.09	0.84 ± 0.06
	0.70–0.81	0.62–0.89	(*N* = 2)	0.69–0.91	0.72–0.92
		(*N* = 21)			
Width of middle phalanx (MPW)					
	0.33 ± 0.03	0.36 ± 0.03	0.40, 0.45	0.43 ± 0.03	0.48 ± 0.03
	0.33–0.36	0.30–0.44	(*N* = 2)	0.41–0.47	0.42–0.52
		(*N* = 21)			
Length of distal phalanx (DPL)					
	0.95 ± 0.07	1.12 ± 0.10	1.28 ± 0.22	1.27 ± 0.06	1.30 ± 0.08
	0.87–1.05	0.82–1.23	1.03–1.46	1.18–1.34	1.18–1.48
		(*N* = 23)			
Width of distal phalanx (DPW)					
	0.42 ± 0.02	0.45 ± 0.04	0.52 ± 0.05	0.55 ± 0.02	0.57 ± 0.03
	0.40–0.46	0.39–0.54	0.46–0.56	0.52–0.59	0.51–0.62
		(*N* = 21)			(*N* = 14)
Length of claw (CL)					
	1.76 ± 0.06	2.08 ± 0.20	2.50 ± 0.27	2.23 ± 0.22	2.24 ± 0.20
	1.69–1.84	1.29–2.33	2.21–2.73	1.98–2.61	2.03–2.73
	(*N* = 6)	(*N* = 10)			
Width of claw (CW)					
	0.26 ± 0.02	0.29 ± 0.02	0.35, 0.36	0.32 ± 0.05	0.34 ± 0.03
	0.25–0.28	0.26–0.33	(*N* = 2)	0.30–0.42	0.30–0.42
	(*N* = 2)	(*N* = 23)			(*N* = 12)

Species are ordered by width of metacarpal.
Statistics are mean ± SD and range.
Variations in sample sizes appear in parentheses.

Table 6. Component loadings on first four factor axes from principal components analysis of ten $\log_{10}$-transformed craniomandibular variables from six species of broad-clawed *Cryptotis*. See Figure 2

	Component loadings			
Variable	1	2	3	4
M2B	0.908	–0.230	0.001	–0.004
HCP	0.905	–0.258	0.031	0.162
ML	0.902	0.031	0.099	0.040
HCV	0.873	–0.188	0.083	0.206
PL	0.844	0.298	0.027	–0.040
TR	0.843	0.436	–0.093	–0.046
PO	0.837	–0.283	–0.127	0.192
M1L	0.692	–0.127	–0.072	–0.685
UTR	0.321	0.883	–0.006	0.088
ZP	0.023	0.013	0.993	–0.054
Eigenvalue	5.924	1.310	1.035	0.590
Percentage of variation	59%	13%	10%	6%

M2B, breadth across second molars; HCP, height of coronoid process; ML, length of mandible; HCV, height of condylar valley; PL, length of palate; TR, length of maxillary toothrow; PO, postorbital breadth; M1L, length of upper first molar; UTR, length of unicuspid toothrow; ZP, breadth of zygomatic plate.

other two Alta Verapaz specimens as well as individuals of *C. goodwini* and *C. magnimanus*; and *C. lacertosus* comprises the subset with the largest humeri. Factor 2 is strongly influenced by the variable MT and, to a lesser extent, CD, but this axis provides no separation amongst species. The Alta Verapaz sample exhibits the greatest range of variation of any taxon along the first axis, but is the most conservative species along the second axis.

Statistical analysis of the humerus confirms that the humerus of the Alta Verapaz sample is distinctly smaller than that of *C. lacertosus* and shows that it averages larger than that of *C. mam*, although the overall size range of the Alta Verapaz sample overlaps the ranges of *C. goodwini*, *C. magnimanus*, and *C. mam*.

Manus variables

External aspects of the forefeet of the six species of broad-clawed shrews from this region vary perceptibly, yet differences between any two species can be subtle. Analysis of variables measured from X-rays of the manus of dried skins permits quantitative assessment of potential differences at a smaller scale than is possible from available skeletons, and it provides substantially larger samples to be used (Woodman & Stephens, 2010).

In my statistical analyses of rays I, III, and V from the five species of broad-clawed shrews, different numbers of variables were analysed for each ray. Despite these differences, the cohesiveness of species and the multivariate spatial relationships amongst species generally remained the same, although the degree of separation amongst groupings of species tended to vary.

Table 7. Component loadings on first four factor axes from principal components analysis of ten $\log_{10}$-transformed craniomandibular variables from the three largest species of broad-clawed *Cryptotis*. See Figure 3

	Component loadings			
Variable	1	2	3	4
HCP	0.887	0.243	–0.132	0.026
M2B	0.865	0.192	0.001	–0.014
HCV	0.839	0.076	–0.288	–0.095
ML	0.747	–0.188	–0.256	0.143
PO	0.737	0.375	–0.149	–0.075
TR	0.571	–0.708	0.230	0.061
PL	0.460	–0.678	0.155	–0.123
M1L	0.332	0.372	0.532	0.670
UTR	0.076	–0.828	0.001	0.165
ZP	–0.396	–0.188	–0.705	0.496
Eigenvalue	4.149	2.099	1.045	0.778
Percentage of variation	41%	21%	10%	8%

HCP, height of coronoid process; M2B, breadth across second molars; HCV, height of condylar valley; ML, length of mandible; PO, postorbital breadth; TR, length of upper maxillary toothrow; PL, length of palate; M1L, length of upper first molar; UTR, length of unicuspid toothrow, ZP, breadth of zygomatic plate.

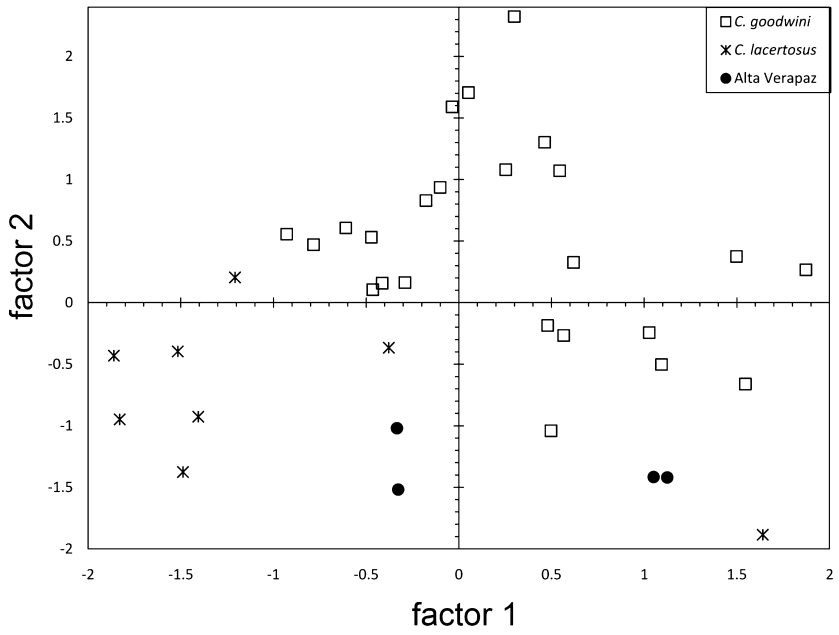

Figure 3. Plot of scores on first two axes from principal components analysis of skulls of the three largest species of broad-clawed *Cryptotis* (see Table 7).

Table 8. Component loadings on first three factors from principal components analysis of seven $\log_{10}$-transformed humerus measurements from five species of broad-clawed *Cryptotis*. See Figure 4

	Component loadings		
Variable	1	2	3
BS1	0.966	–0.098	–0.005
L1	0.956	0.197	0.044
DW	0.951	0.148	0.148
PW	0.949	0.015	0.251
GT	0.941	–0.166	0.071
CD	0.757	0.465	–0.455
MT	–0.570	0.778	0.242
Eigenvalue	5.438	0.921	0.358
Percentage of variation	77.7%	13.2%	5.1%

BS1, breadth of shaft; L1, length; DW, width; PW, proximal width; GT, distal greater tuberosity to teres tubercle; CD, deltoid process to capitulum; MT, medial epicondyle to teres tubercle.

In a plot of factor scores from the PCA of ray I, there is separation along factor 1 axis (size – Table 9A, Fig. 5A) between a subset of species with smaller ray I bones (*C. griseoventris*, *C. mam*) and a second subset with larger bones (*C. goodwini*, *C. lacertosus*). The two specimens comprising the Alta Verapaz sample bridge the gap between the two size subsets. All variables load out positively on factor 1, with widths of bones consistently more strongly weighted, and thereby more influential, than lengths (Table 9A). Factor 2 is a contrast of ML and PPL with MW, and along this axis, *C. lacertosus* averages lower values (shorter and wider metacarpal), and the Alta Verapaz samples averages larger values (longer and narrower metacarpal), than *C. goodwini*.

The clearest separation amongst taxa is provided by the PCA of ray III (Fig. 5B). In the plot of factor scores from this analysis, there are three distinct subsets along the factor 1 axis, which represents size, with widths and DPL more strongly weighted than lengths of other bones (Table 9B). Three size classes are discernible: the class representing the smallest ray I bones is represented by *C. griseoventris*; the intermediate class is comprised of *C. mam*; the large size class includes *C. goodwini* and *C. lacertosus*. As with ray I, the Alta Verapaz sample bridges the gap in size between the intermediate and large size classes. Factor 2 primarily represents a negatively weighted ML, with a small contribution from PPL and a weak contrast with MW. Along the second factor axis, the Alta Verapaz sample averages lower scores (longer metacarpals) than the other four species, indicating a tendency for longer metacarpals. In fact, the ray III metacarpals of this species average both longer and narrower than those of *C. goodwini* and *C. lacertosus* (Fig. 6; Table 4).

In a plot of factor scores from the PCA of ray V, the order of taxa along factor axis 1 (size – Table 9C,

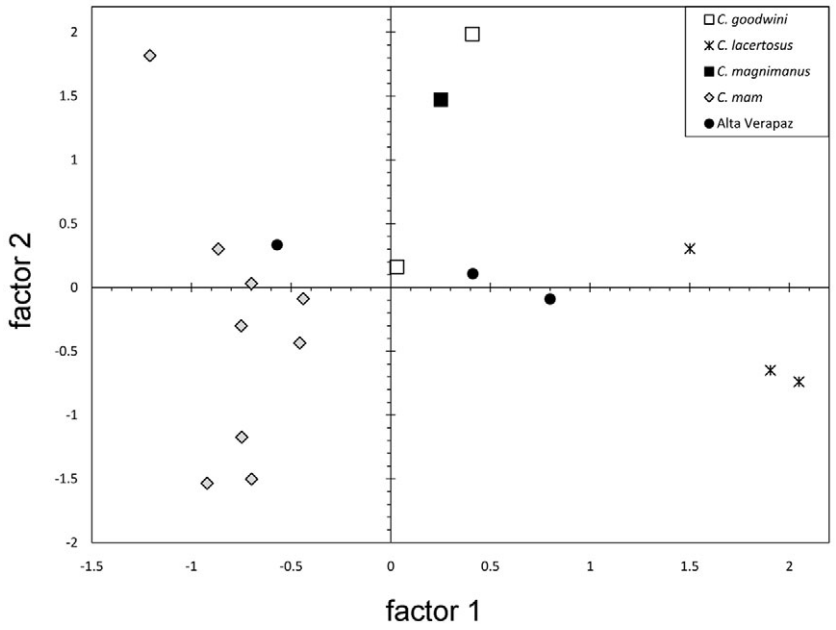

Figure 4. Plot of scores on first two axes from principal components analysis of humeri of five species of broad-clawed *Cryptotis* (see Table 8).

Fig. 5C) is the same as in that in the PCA plot for ray III, but only two size classes are apparent instead of three: the smaller size class is represented by *C. griseoventris*, *C. mam*, and the larger by *C. goodwini* and *C. lacertosus*. As in the plots for the other two rays, the Alta Verapaz sample bridges the gap in size between the two subsets of species. Factor 2 represents a negatively weighted MPL, but there is no separation of taxa along this axis.

In summary, rays I, III, and V of the Alta Verapaz sample are larger than those of *C. griseoventris* and smaller individuals of *C. mam*. They are comparable in size to those of *C. goodwini*, *C. lacertosus*, and the larger *C. mam*. The Alta Verapaz sample has longer and narrower metacarpals of ray I and longer metacarpals of ray III than both *C. goodwini* and *C. lacertosus*.

Cluster analyses

Topologies amongst distance trees resulting from cluster analyses varied considerably amongst data sets. Missing data on the humerus of *C. griseoventris* and on the manus of *C. magnimanus* probably affected results of some analyses, but the varying topologies also reflect different degrees of differentiation within morphological structures.

The distance tree resulting from analysis of 21 skull variables divides the six species into two groups, one comprised of *C. griseoventris*, *C. magnimanus*, and *C. mam*; the other of *C. lacertosus*, *C. goodwini*, and the Alta Verapaz sample (Fig. 7A). Within the latter group, the Alta Verapaz sample is most similar to *C. lacertosus*.

The cluster diagram from analysis of seven humerus variables (Fig. 7B) differs considerably from that based on the skull. In the humerus tree, the groups of species reflect the three size classes observed in the PCA of humeri (Fig. 4), but the tree does not preserve the order of smallest to largest. The Alta Verapaz sample is most similar to the pairing of *C. goodwini* and *C. magnimanus*. In the PCA, these three species all had primarily medium-sized humeri. Further removed from these three species is *C. mam*, the species with the smallest and least modified humerus. *Cryptotis lacertosus*, which has the largest humerus, appears in the tree as the most distant and distinctive species.

Cluster trees for the individual rays exhibit two distinct patterns. In each one, however, *C. goodwini* and *C. lacertosus* are paired as most similar to each other. In the tree for ray I, the Alta Verapaz sample is basal and most distinct from the other four species, which form two pairs: the *C. goodwini*/*C. lacertosus* pair and a *C. griseoventris*/*C. mam* pair (Fig. 7C). The two cluster trees for ray III and ray V are topologically identical to each other, although distances separating groups vary substantially (Fig. 7D, E). In these diagrams, the basal species is *C. griseoventris*, and the Alta Verapaz sample is most similar to the *C. goodwini*/*C. lacertosus* pair. In a cluster tree combining the variables from all three rays (Fig. 7F), the

Table 9. Component loadings on first four factors from principal components analysis of individual rays from five species of broad-clawed *Cryptotis*: A, six $\log_{10}$-transformed variables from ray I; B, eight $\log_{10}$-transformed variables from ray III; C, six $\log_{10}$-transformed variables from ray V. See Figure 5

	Component loadings			
Variable	1	2	3	4
A				
1PPW	0.911	–0.152	0.091	0.070
1DPW	0.899	–0.243	0.062	0.031
1MW	0.809	–0.515	–0.012	0.107
1DPL	0.691	0.233	–0.309	–0.609
1PPL	0.588	0.520	–0.452	0.421
1ML	0.571	0.537	0.614	–0.008
Eigenvalue	3.442	0.961	0.689	0.566
Percentage of variation	57.3%	16.0%	11.5%	9.4%
B				
3PPW	0.945	0.133	0.045	–0.104
3DPW	0.938	0.134	0.042	0.039
3MPW	0.931	0.074	0.056	–0.243
3DPL	0.895	0.081	–0.016	0.055
3MW	0.894	0.368	0.066	–0.033
3PPL	0.687	–0.407	0.451	0.386
3MPL	0.550	–0.075	–0.795	0.227
3ML	0.484	–0.827	–0.104	–0.252
Eigenvalue	5.250	1.038	0.858	0.340
Percentage of variation	65.6%	13.0%	10.7%	4.2%
C				
5DPW	0.954	0.026	0.040	–0.063
5MPW	0.927	–0.152	0.109	0.221
5PPW	0.909	–0.063	0.322	0.115
5DPL	0.880	0.307	0.078	–0.324
5PPL	0.756	0.354	–0.535	0.113
5MPL	0.417	–0.870	–0.231	–0.117
Eigenvalue	4.116	1.004	0.462	0.198
Percentage of variation	68.6%	16.726	7.7%	3.3%

PPW, width of proximal phalanx; DPW, width of distal phalanx; MPW, width of middle phalanx; DPL, length of distal phalanx; MW, width of metacarpal; PPL, length of proximal phalanx; MPL, length of middle phalanx; ML, length of metacarpal.

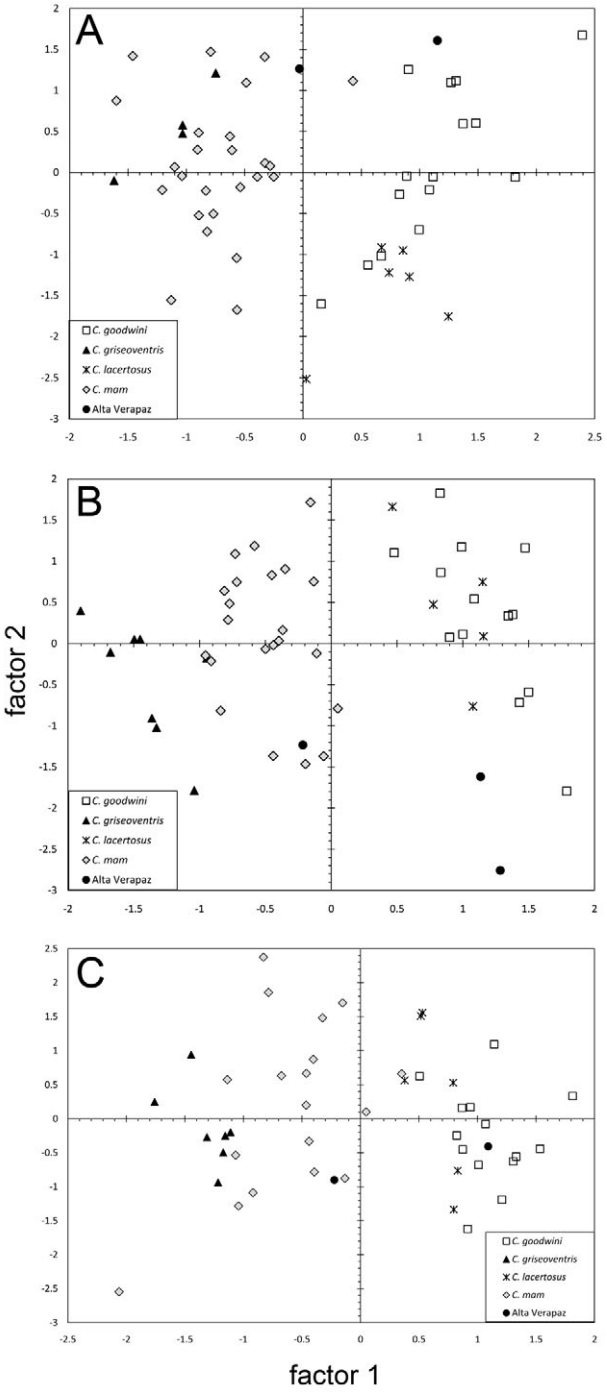

Figure 5. Plots of scores on first two axes from principal components analyses of individual rays from five species of broad-clawed *Cryptotis*: A, six variables from ray I; B, eight variables from ray III; C, six variables from ray V (see Table 9).

Alta Verapaz sample is basal, as in the tree for ray I, but relationships amongst the other four species are different. In this tree, the *C. lacertosus*/*C. goodwini* pair is most similar to *C. mam*, and these three species are most similar to *C. griseoventris*.

The tree resulting from cluster analysis of all 59 variables (Fig. 7G) is unlike any of the trees for the individual sets of variables. In this tree, the Alta Verapaz sample is most similar to *C. lacertosus*, and this pair is grouped with *C. goodwini*. *Cryptotis griseoventris* and *C. mam* form a second pair, whereas *C. magnimanus* is the most basal species.

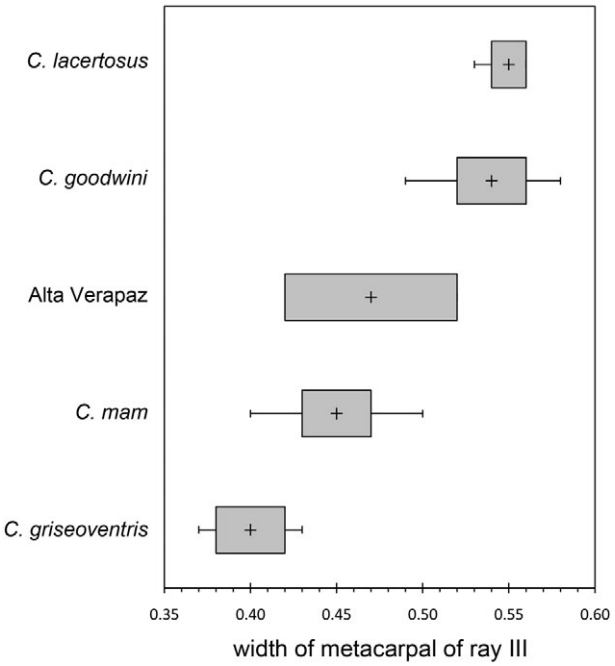

Figure 6. Box-and-whisker plot of width of metacarpal of ray III for five species of broad-clawed *Cryptotis*. Cross within each box represents the mean, shaded box indicates SD, and vertical line shows the range of values for each species.

Cluster analyses show patterns of overall similarity rather than any implicit indication of genetic relatedness, particularly given the nature of metrical data. In this case, the Alta Verapaz sample is morphometrically most similar to *C. lacertosus* overall. Yet, individual cluster analyses suggest that the skull of the Alta Verapaz sample is most similar to that of *C. lacertosus*; the humerus is most similar to those of *C. goodwini* and *C. magnimanus*; ray III and ray V are most similar to those of *C. goodwini* and *C. lacertosus*; and ray I is distinctive from all of the other species. My interpretation of the different patterns exhibited by trees based on variables from different morphological structures is that, at the species level, these structures are evolving at least partly in independence of one another, despite some close correspondence in function (e.g. humerus and forefeet as adaptations for digging).

Systematic biology

Family Soricidae Fischer, 1814

Genus *Cryptotis* Pomel, 1848

Cryptotis oreoryctes sp. nov. (Figs 9F, 10E)

Cryptotis parva tropicalis: Choate, 1970: 269. Part; not *Cryptotis parvus tropicalis* (Merriam, 1895).

Holotype: Dried skin, skull, and partial skeleton of adult female, USNM 569877; obtained 4.i.2007 by N. Woodman (John O. Matson field number 7288) in the Chelemhá Cloud Forest Reserve (*c.* 15°23′N, 90°04′W), *c.* 2090 m.a.m.s.l., Alta Verapaz, Guatemala.

Paratypes (six individuals)*:* All from Alta Verapaz, Guatemala: dried skins, skulls, and partial skeletons of a young male obtained 2.i.2007 (USNM 569854) and an adult female obtained 3.i.2007 (USNM 569878) from the type locality; cranium (but not the associated skin or mandibles, which belong to a younger *C. merriami*) of an old adult of unknown sex (BMNH 43.9.15.4) and a previously mounted skin with glass eyes (BMNH 43.9.15.5) and separately numbered skull (BMNH 43.10.28.7) of a young adult of unknown sex obtained in the mid-19th century from 'near Coban' and provided to BMNH by specimen dealer John Leadbeater; dried skins and skulls of two young adults of unknown sex obtained in the mid-19th century by Osbert Salvin from 'Verapaz' (BMNH 68.2.10.5) and from 'near Coban' (BMNH7.1.1.35). See Woodman (2011) for additional details regarding the history of BMNH specimens.

Distribution: Known with certainty only from the vicinity of the type locality (Fig. 8). The species is probably restricted to remaining forest patches at higher elevations throughout the Sierra de Yalijux. Nineteenth-century specimens in the BMNH from 'Coban' may have been taken in forests at higher elevations to the east of that city, Cobán being the closest contemporary population centre of any size.

Etymology: The species name *oreoryctes* is derived from the classical Greek words *ορος* ('mountain') + *ορυσσω* ('to dig') and signifies 'digging in the mountains'.

Diagnosis: As a broad-clawed shrew of the *C. goldmani* group, *C. oreoryctes* can be distinguished from most other species in the genus by its broad manus and extremely long, broad foreclaws; uncrowded upper unicuspid row in which U^4 is typically aligned and partially visible in labial (fourth unicuspid) view of the rostrum; protoconal basin of M^1 (upper first molar) reduced relative to hypoconal basin; entoconid of M_3 (lower third molar) vestigial or absent; broad humerus with elongated processes (Fig. 9F); short, wide metacarpals and proximal and middle phalanges (Fig. 10E); elongate and broad distal phalanges. Within the *C. goldmani* group, *C. oreoryctes* is distinguished by its dark pelage [paler in *C. alticola* (Merriam, 1895), *C. goldmani* (Merriam, 1895), *C. lacertosus*, *C. magnimanus*, *C. mam*, *C. peregrinus* (Merriam, 1895)]; large external body size (larger than *C. goldmani*, *C. griseoventris*, *C. mam*, *C. peregrinus*); longer tail (longer than in *C. alticola*,

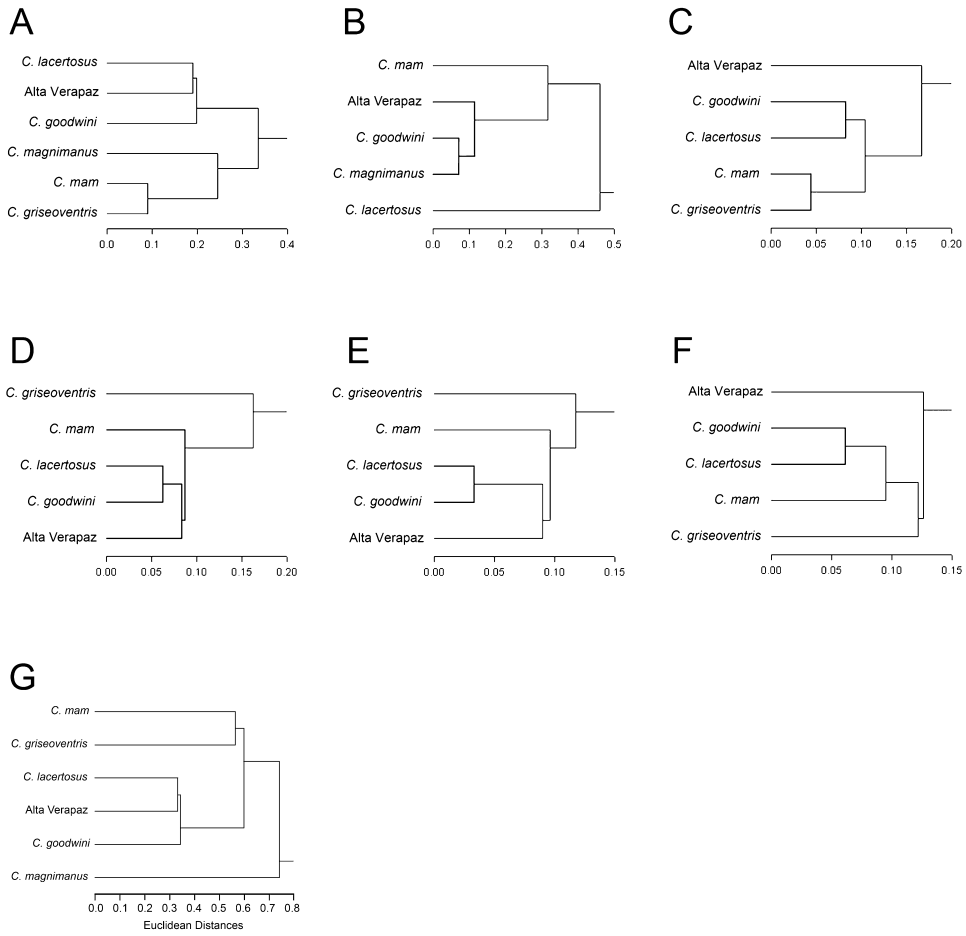

Figure 7. Distance trees resulting from cluster analyses of morphological data sets derived from six species of broad-clawed *Cryptotis*: A, 21 craniomandibular variables; B, seven humerus variables; C, eight variables from ray I; D, ten variables from ray III; E, ten variables from ray V; F, combined analyses of 28 forefoot variables; G, combined analysis of 59 variables.

C. magnimanus); long skull (longer than in *C. alticola*, *C. goldmani*, *C. griseoventris*, *C. magnimanus*, *C. mam*, *C. peregrinus*); relatively long unicuspid row (longer than in *C. alticola*, *C. goldmani*, *C. lacertosus*, *C. magnimanus*, *C. mam*, *C. peregrinus*; but shorter than in *C. griseoventris*); moderately broad palate (relatively broader than in *C. griseoventris* but relatively narrower than in *C. alticola*, *C. goodwini*, *C. lacertosus*, *C. magnimanus*); no foramen of the sinus canal (present in *C. goldmani*, *C. peregrinus*); distinct foramen present on tympanic process of one or both petromastoids (absent in *C. alticola*, *C. goldmani*, *C. goodwini*, *C. griseoventris*, *C. lacertosus*, *C. magnimanus*, *C. mam*, *C. peregrinus*); relatively low coronoid process of mandible (lower than in *C. goldmani*, *C. goodwini*, *C. magnimanus*, *C. peregrinus*); vestigial entoconid of M_3 sometimes present (always absent in *C. griseoventris*, *C. mam*, *C. lacertosus*); broad metacarpal and phalanges of ray III of forefoot (broader than in *C. griseoventris*, *C. mam*, *C. peregrinus*, but narrower than in *C. goodwini*, *C. lacertosus*; Figs 6, 10); long metacarpal of ray III (longer than in *C. goldmani*, *C. goodwini*, *C. griseoventris*, *C. lacertosus*, *C. mam*); long, broad foreclaws (longer and broader than in *C. griseoventris*, *C. mam*, *C. peregrinus*); long, broad humerus with prominent teres tubercle and medial and lateral epicondyles (longer and broader than in *C. alticola*, *C. mam*, *C. peregrinus*; longer than in *C. goldmani*, but not as obviously massive as *C. lacertosus*).

Description: A large member of the genus *Cryptotis* with a relatively short tail, averaging 30 mm, or 36 ± 3% of head-and-body length (Tables 1, 10); forefeet broad, foreclaws long and broad. Dorsal pelage approximates Fuscous Black to Chaetura Black; dorsal guard hairs typically 5–6 mm long, with individual hairs up to 7 mm, and indistinctly two-banded: basal five-sixths of hairs silvery grey, grading to a dark brown tip. Ventral pelage paler than dorsum:

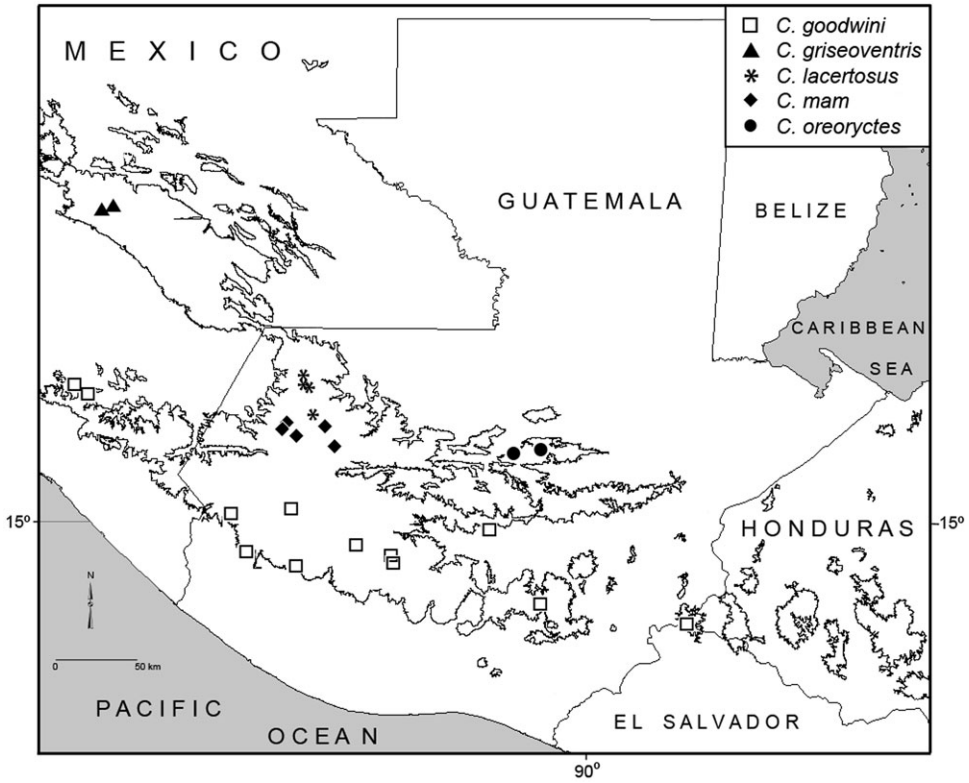

Figure 8. Map of southern Mexico and northern Central America, indicating the distributions of five species of broad-clawed *Cryptotis*. Contour represents 1500 m.a.m.s.l..

Mummy Brown to Van Dyke Brown to Sepia. Rostrum long (PL/CBL = 44.5 ± 0.2%; Table 10); postorbital area broad (PO/CBL = 25.9 ± 0.7%); often two obvious dorsal foramina (67%) on the frontals; no ventral extension of the sinus canal or associated foramen posterior to dorsal mandibular articular facet of the skull; typically an obvious foramen dorsal to the dorsal mandibular articular facet present on one or both sides of the skull (100%); typically a distinct foramen on the posteromedial edge of tympanic process of one or both petromastoids [100%; this foramen is much smaller than in *C. colombiana* Woodman & Timm, 1993, or *C. thomasi* (Merriam, 1897b) – see Woodman & Timm, 1999]; zygomatic plate highly variable in this species, but more typically relatively short (ZP/PL = 21.7 ± 2.9%); anterior border of zygomatic plate typically aligned with mesostyle–metastyle valley or metastyle of M^1, posterior border aligned with posterior edge of M^3 (upper third molar), and at the posterior root of the maxillary process; palate of medium breadth for the genus (M2B/PL = 65.7 ± 1.4%); upper toothrow uncrowded; dentition not bulbous; upper molars lightly to moderately pigmented: medium red to dark red on tips of cones, styles, and cristae; pale to medium red pigment often extends into protoconal basins (67%), and paler red into hypoconal basins, of M^1 and M^2 (upper second molar); unicuspid toothrow relatively long (UTR/CBL = 13.6 ± 0.1%); posteroventral borders of unicuspids variable, concave to convex; U^4 aligned with the unicuspid row and typically visible in labial view of the rostrum; P^4 (upper fourth premolar), M^1, and M^2 slightly recessed on posterior border; protoconal basin of M^1 reduced relative to hypoconal basin. M^3 small and simple: pigmented parastyle, paracrista, and paracone; reduced precentrocrista and mesostyle may or may not be pigmented; often a short postcentrocrista present; reduced protocone may or may not be pigmented; metacone absent; vestigial, unpigmented hypocone occasionally present. Mandible relatively long and of moderate breadth for the genus; coronoid process of mandible intermediate in height (HCP/ML = 69.7 ± 1.6%); anterior border of the coronoid process of the mandible joining horizontal ramus at a relatively low angle; long distance from the superior tip of articular process to the posterior border of M_3 (AC3/ML = 80.5 ± 4.1%); articular process generally moderately tall and wide, with a moderately broad lower articular facet; inferior sigmoid notch deep; posterior border of lower incisor aligned approximately with posterior border of hypoconid of P_4 (lower fourth premolar); P_3 (lower third

Figure 9. Anterior aspect of left humeri of A, *Cryptotis parvus parvus* (USNM 582437); B, *Cryptotis mexicanus* (USNM 29541); C, *Cryptotis mam* (USNM 570340); D, *Cryptotis goodwini* (USNM 275681); E, *Cryptotis goodwini* (UMMZ 103416); F, *Cryptotis oreoryctes* (USNM 569877); G, *Cryptotis lacertosus* (USNM 569503).

premolar) relatively long and low; entoconid of M_3 vestigial or absent. Metacarpals and proximal and middle phalanges relatively short and broad (Table 2); distal phalanges elongate and broad; humerus considerably shortened and broadened with elongate processes (Fig. 7) and dorsoventrally elongate head; medial epicondyle of humerus hooked dorsally; posterior edge of falciform process of the tibia with a deep sulcus.

Comparisons

Like most other members of the *C. goldmani* group, *C. oreoryctes* can be most easily distinguished from Guatemalan members of the *C. parvus* group (i.e. *C. tropicalis*) and *C. nigrescens* group (i.e. *C. mayensis*, *C. merriami*) by its much larger body size (mean HB for *C. tropicalis* = 68 ± 7; *C. mayensis* = 69 ± 7; *C. merriami* = 69 ± 4); longer pelage; broader forefeet and longer, broader foreclaws (Fig. 10); greater skull size (mean CBL for *C. tropicalis* = 17.8 ± 6; *C. mayensis* = 19.2 ± 0.5; *C. merriami* = 19.5 ± 0.4); and broader, more robust humerus with longer processes (Fig. 9). For additional measurements and characters of those species, see Woodman & Timm (1992, 1993).

Amongst members of the *C. goldmani* group in Guatemala and Chiapas (*C. goodwini*, *C. griseoventris*, *C. lacertosus*, *C. mam*), *C. oreoryctes* has approximately the same external body size as *C. lacertosus* (Table 1). Externally, the manus is intermediate in size between those of *C. mam* and *C. goodwini*, and the foreclaws are within the size range of those of *C. goodwini*. Ranges of measurements for individual bones of the forefeet overlap those of *C. mam*, *C. lacertosus*, and *C. goodwini*. Proportionally, however, the metacarpals, proximal phalanges, and distal phalanges of *C. oreoryctes* tend to be relatively long and narrow (Tables 3–5). The humerus of the new species is similar in size and in the prominence of its processes to that of *C. goodwini* (Fig. 9).

Measurements and indices for *C. oreoryctes*, *C. goodwini*, *C. griseoventris*, *C. lacertosus*, and *C. mam* are provided in Tables 1 and 10. Measurements for other species to which *C. oreoryctes* is compared are provided in parentheses. Additional measurements and characters can be found in Woodman & Timm (1999, 2000), Woodman & Morgan (2005), and Woodman (2010).

Cryptotis alticola: Cryptotis oreoryctes averages larger in body size (*C. alticola*: HB = 79 ± 5; WT = 11 ± 3 g) and has a longer tail (*C. alticola*: TL = 26 ± 2;

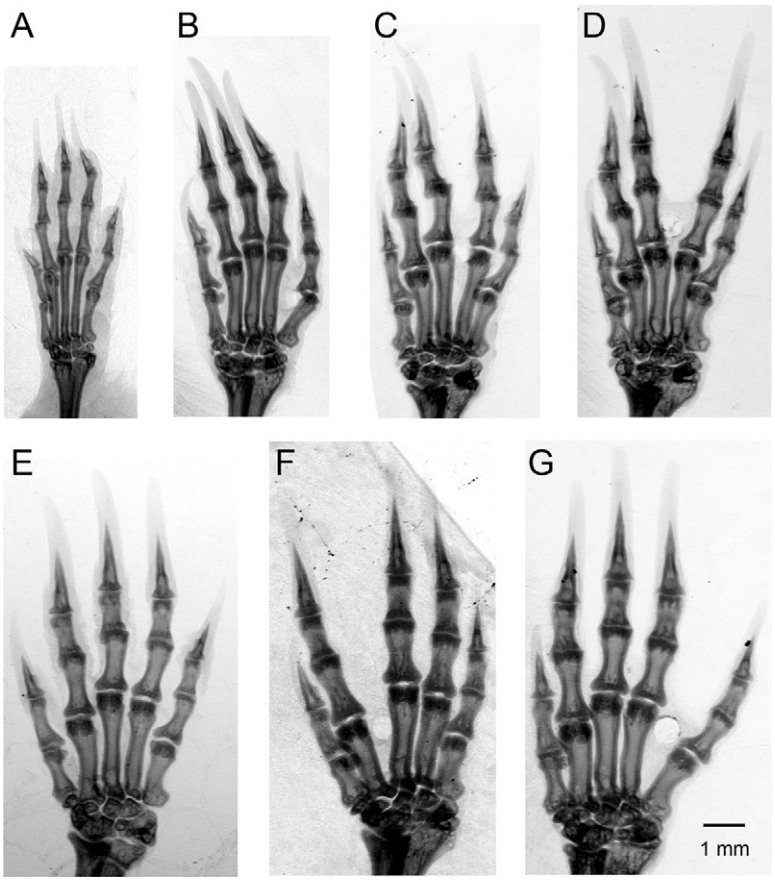

Figure 10. X-ray images of left mani of: A, *Cryptotis parvus parvus* (USNM 568977); B, *Cryptotis mexicanus* (USNM 68298); C, *Cryptotis griseoventris* (USNM 758905); D, *Cryptotis mam* (USNM 77057); E, *Cryptotis oreoryctes* (USNM 569854); F, *Cryptotis lacertosus* (USNM 569442); G, *Cryptotis goodwini* (USNM 77078).

TL/HB = 33 ± 4%). The forefeet are of similar size, but the foreclaws are broader. *Cryptotis oreoryctes* averages larger in skull size (*C. alticola*: CBL = 20.2 ± 0.5; BB = 10.4 ± 0.2); has a relatively longer rostrum (*C. alticola*: PL/CBL = 43.2 ± 1.2%); relatively narrower palate (*C. alticola*: M2B/PL = 70.9 ± 3.0%); and a longer unicuspid row (*C. alticola*: UTR = 2.5 ± 0.1; UTR/CBL = 12.3 ± 0.4%). *Cryptotis oreoryctes* lacks a vestigial foramen of the sinus canal (present in 52% of *C. alticola*) and tends to have an obvious foramen dorsal to the dorsal articular facet for the mandible (present in 39% of *C. alticola*). Its humerus tends to be shorter, but relatively broader with longer processes than that of *C. alticola*. *Cryptotis alticola* is endemic to highlands of central Mexico.

Cryptotis goldmani: Cryptotis oreoryctes averages larger in body size (*C. goldmani*: HB = 76 ± 5; WT = 8 ± 1). The forefeet are longer and narrower, and the foreclaws are shorter and narrower. *Cryptotis oreoryctes* averages larger in skull size (*C. goldmani*: CBL = 19.6 ± 0.5; BB = 10.2 ± 0.2); has a longer unicuspid row (*C. goldmani*: UTR = 2.3 ± 0.1; UTR/CBL = 11.9 ± 0.6%); longer and broader palate (*C. goldmani*: PL = 8.7 ± 0.3; M2B = 5.8 ± 0.1); and relatively low coronoid process (*C. goldmani*: HCP/ML = 80.5 ± 2.6%). *Cryptotis oreoryctes* lacks a foramen of the sinus canal (well developed in *C. goldmani*) and typically has an obvious foramen dorsal to the dorsal articular facet (present in 16% of *C. goldmani*). Its humerus is longer, and the processes, particularly teres tubercle and medial epicondyle, are proportionately shorter, but broader. The bones of the forefoot average longer and slightly broader; in ray III, however, the metacarpal averages much longer (*C. goldmani*: ML = 2.67 ± 0.28) and the middle phalanx much shorter (*C. goldmani*: MPL = 1.09 ± 0.27). *Cryptotis goldmani* is endemic to highlands in the Mexican states of Guerrero and Oaxaca.

Cryptotis goodwini: Cryptotis oreoryctes averages smaller in body size. The manus is smaller overall, and the foreclaws are shorter and much narrower.

Table 10. Comparison of characters amongst six species of broad-clawed *Cryptotis*

	Cryptotis griseoventris (*N* = 8)	*Cryptotis mam* (*N* = 22)	*Cryptotis magnimanus* (*N* = 1)	Alta Verapaz (*N* = 3)	*Cryptotis lacertosus* (*N* = 8)	*Cryptotis goodwini* (*N* = 19)
Relative length of tail (TL/HB × 100)	38 ± 3 34–42 (*N* = 10)	38 ± 3 33–44 (*N* = 28)	31	36 ± 3 33–39	34 ± 4 28–40	35 ± 3 30–41 (*N* = 32)
Relative breadth of interorbital area (PO/CBL × 100)	25.4 ± 0.7 24.2–26.1	25.9 ± 0.8 24.3–27.6	26.1	25.9 ± 0.7 25.1–26.5	24.6 ± 0.2 24.3–25.0	26.6 ± 0.9 25.2–28.1
Relative length of rostrum (PL/CBL × 100)	44.5 ± 0.6 43.5–45.5	43.5 ± 0.9 42.1–45.0	43.3	44.5 ± 0.2 44.2–44.7	43.5 ± 0.8 42.1–44.7	43.7 ± 0.7 42.5–44.8
Relative breadth of zygomatic plate (ZP/CBL × 100)	9.6 ± 0.6 9.0–10.8	9.8 ± 0.6 8.0–10.4	10.8	9.7 ± 0.2 9.5–9.8	9.7 ± 1.2 7.9–11.8	9.2 ± 0.8 7.4–10.8
Relative breadth of zygomatic plate (ZP/PL × 100)	21.6 ± 1.5 20.0–24.4	22.4 ± 1.4 18.2–24.7 (*N* = 26)	25.0	21.7 ± 2.9 17.6–26.7 (*N* = 7)	22.4 ± 3.0 17.8–27.2	21.1 ± 1.6 17.2–24.4 (*N* = 24)
Relative length of unicuspid row (UTR/CBL × 100)	13.9 ± 0.5 13.1–14.5	13.5 ± 0.3 12.9–14.1	11.8	13.6 ± 0.1 13.5–13.7	13.0 ± 0.3 12.6–13.6	13.0 ± 0.5 12.0–14.0
Relative breadth of palate (M2B/PL × 100)	62.9 ± 1.6 60.7–65.1	65.2 ± 1.6 61.4–68.2 (*N* = 26)	67.1	65.7 ± 1.4 63.8–67.4	63.6 ± 1.5 62.4–66.7	68.2 ± 2.0 64.2–71.6 (*N* = 24)
Relative height of coronoid process (HCP/ML × 100)	69.0 ± 1.9 65.6–72.9 (*N* = 10)	71.7 ± 2.3 67.2–76.3 (*N* = 28)	72.3	69.7 ± 1.6 68.1–72.1 (*N* = 5)	71.2 ± 2.2 69.2–76.2	72.4 ± 2.0 68.7–76.5 (*N* = 25)
Relative posterior length of mandible (AC3/ML × 100)	81.6 ± 2.2 79.7–86.4 (*N* = 10)	83.6 ± 2.3 78.1–87.3 (*N* = 28)	81.5	80.5 ± 4.1 76.1–85.3 (*N* = 4)	84.1 ± 3.7 79.7–90.5	83.5 ± 2.7 77.9–87.3 (*N* = 25)
Relative extension of articular condyle (AC3/HCP × 100)	118.3 ± 2.6 114.0–121.4 (*N* = 10)	116.8 ± 5.0 104.2–127.9 (*N* = 28)	112.8	115.2 ± 4.1 110.9–120.8 (*N* = 4)	118.0 ± 3.5 113.3–124.4	115.4 ± 4.5 108.2–125.5 (*N* = 25)
Foramen of sinus canal (present)	0% (*N* = 10)	0% (*N* = 25)	0%	0% (*N* = 3)	0% (*N* = 6)	17% tiny (*N* = 12)
Foramen dorsal to dorsal articular facet (present)	90% (*N* = 10)	96% (*N* = 25)	100%	100% (*N* = 3)	50% (*N* = 6)	100% (*N* = 14)
Two obvious dorsal foramina (present)	100% (*N* = 10)	88% (*N* = 25)	100%	66% (*N* = 3)	100% (*N* = 6)	80% (*N* = 15)
Distinct foramen on tympanic process of one or both petromastoids	13% Tiny (*N* = 8)	21% Tiny to small	0%	100% Small to large (*N* = 3)	0% (*N* = 6)	25% Tiny to small (*N* = 12)
Posteroventral border of unicuspids	Concave	Concave	Concave	Concave to convex	Concave	Concave to convex
Vestigial entoconid of M_3 (present)	0% (*N* = 10)	0% (*N* = 25)	?	50% (*N* = 2)	0% (*N* = 5)	8% (*N* = 12)

Abbreviations of variables as in Table 1.
Statistics are mean ± SD and range.

Cryptotis oreoryctes averages a longer, narrower skull (Table 1 – CBL, BB, PO); broader zygomatic plate; longer toothrow; relatively short coronoid process of the mandible; and relatively short posterior length of the mandible. The humerus is generally similar to that of *C. goodwini* (Table 2; Fig. 9). Ray III of the forefoot averages longer and narrower; the middle and distal phalanges, however, are shorter (Table 4; Fig. 6). *Cryptotis goodwini* occurs in highlands from Chiapas, Mexico, to Honduras.

Cryptotis griseoventris: Cryptotis oreoryctes averages larger externally (Table 1), and the forefeet appear larger, with longer, broader foreclaws. It also averages larger in nearly all craniomandibular measurements; has a relatively broad palate (Table 10); more likely to have broad unicuspids with a more convex posteroventral surface; and more likely to possess a vestigial entoconid on M_3. The humerus of *C. griseoventris* is unknown. The bones and claws of the forefoot are longer and broader (Table 4; Fig. 6). *Cryptotis griseoventris* is endemic to northern highlands of Chiapas, Mexico.

Cryptotis lacertosus: Cryptotis oreoryctes has distinctly darker pelage. It averages nearly as large in external measurements, but the manus is smaller, and the foreclaws are shorter and narrower. *Cryptotis oreoryctes* averages nearly as large in skull size (Table 1), but has a relatively long rostrum (Table 10); relatively broad palate; longer toothrow; longer mandible; relatively short posterior length of the mandible. It more often has broad unicuspids with a more convex posteroventral surface, and it is more likely to possess a vestigial entoconid on M_3. The humerus of *C. oreoryctes* is shorter and less massive (Table 2; Fig. 9). Most metacarpals and phalanges of the forefoot are longer and often narrower; the middle phalanx of ray III, however, is shorter (Table 4; Fig. 6). *Cryptotis lacertosus* is endemic to the northern Sierra de los Cuchumatanes of western Guatemala.

Cryptotis magnimanus: Cryptotis oreoryctes has distinctly darker pelage. It averages nearly as large in external measurements, but the tail is shorter. *Cryptotis oreoryctes* has a longer skull (Table 1), relatively long rostrum and narrow palate (Table 10); longer maxillary and unicuspid toothrows; longer mandible and mandibular toothrow. It more often has broad unicuspids with a more convex posteroventral surface. *Cryptotis magnimanus* is known only from the Cordillera de Montecillos of Honduras.

Cryptotis mam: Cryptotis oreoryctes has distinctly darker pelage and averages larger in head-and-body length (Table 1), but tends to have a relatively short tail (Table 10). Its manus is larger externally, and the foreclaws narrower. *Cryptotis oreoryctes* averages larger in nearly all craniomandibular measurements. It averages a longer rostrum; relatively shorter posterior length of the mandible; broader unicuspids with a more convex posteroventral surface; and it is more likely to possess a vestigial entoconid on M_3. The humerus is larger and more massive, with more prominent teres tubercle and epicondyles (Table 2; Fig. 9). The bones and claws of the forefoot are longer and broader (Table 3–5; Fig. 6). *Cryptotis mam* is endemic to the Sierra de los Cuchumatanes, western Guatemala.

Cryptotis peregrinus: Cryptotis oreoryctes is larger (*C. peregrinus*: HB = 72 ± 3), but has a relatively short tail (*C. peregrinus*: TL/HB = 42% ± 3); larger forefeet and longer, broader foreclaws. It also averages larger in nearly all craniomandibular measurements (*C. peregrinus*: CBL = 19.1 ± 0.4; BB = 9.9 ± 0.1; M2B = 5.5 ± 0.2); and has a relatively long zygomatic plate (*C. peregrinus*: ZP/PL = 19.3% ± 1.0); relatively long unicuspid toothrow (*C. peregrinus*: UTR/CBL = 12.9% ± 0.3); and relatively low coronoid process of the mandible (*C. peregrinus*: HCP/ML = 73.1% ± 1.6). *Cryptotis oreoryctes* tends to have broader unicuspids with a more convex posteroventral surface; lacks a sinus canal and associated foramen (well developed in 94% of *C. peregrinus*); and typically has an obvious foramen dorsal to the dorsal articular facet (foramen present in 13% of *C. peregrinus*). The humerus is larger and more massive, with more prominent teres tubercle and epicondyles. *Cryptotis peregrinus* is endemic to highlands in central and western Oaxaca, Mexico.

Remarks

The holotype and two other individuals of *C. oreoryctes* were captured on a steep, moist, north-facing slope with abundant downed trees and mosses in a cloud forest dominated by oaks, pines, and firs at Chelemhá Cloud Forest Reserve in the Sierra de Yalijux. This site is in a region in which native vegetation is classified as Subtropical Montane Rain Forest (Holdridge, 1947; MAGA, 2001). Chance of frost (Tamasiunas *et al.*, 2002) at higher elevations in the Sierra de Yalijux varies from low (2–10%) to moderate (20–50%).

The Chelemhá cloud forest contains a diverse association of small mammals. Based on captures using a combination of Sherman live traps, Museum Special snap traps, and pit-falls over seven nights (*c.* 3208 trap-nights), the small mammal community includes at least 15 species. It is dominated numerically by

Peromyscus grandis Goodwin, 1932 and secondarily by *Oryzomys saturatior* Merriam, 1901a. *Heteromys desmarestianus* Gray, 1868, *Oligoryzomys fulvescens* (Saussure, 1860), *Reithrodontomys mexicanus* (Saussure, 1860), *Scotinomys teguina* (Alston, 1877a), and *Sorex veraepacis veraepacis* Alston, 1877b are relatively abundant (ten to 20 captures) members of the community, whereas *Marmosa mexicana* Merriam, 1897a, *Nyctomys sumichrasti* (Saussure, 1860), *Peromyscus aztecus* (Saussure, 1860), *Peromyscus beatae* Thomas, 1903, *Reithrodontomys microdon* Merriam, 1901b, *Reithrodontomys sumichrasti* (Saussure, 1861), *Reithrodontomys tenuirostris* Merriam, 1901b, and *Cryptotis oreoryctes* are less common (< ten captures).

Reproductive biology of *C. oreoryctes* is poorly known. A female with obviously worn dentition was pregnant with three embryos on 4 January. A younger female captured on the same day was parous, but not pregnant. The testes of a young male with nearly unworn dentition that was captured on 3 January measured 2.5×2 mm.

ACKNOWLEDGEMENTS

I thank the Consejo Nacional de Areas Protegidas (CONAP), Guatemala, for providing collection permits and other valuable assistance. The Unión para Proteger el Bosque Nuboso (UPROBON) graciously granted permission to work in Chelemhá Cloud Forest Reserve. Walter Bulmer, Ralph P. Eckerlin, John O. Matson, Nicté Ordónez, and John Hanson were invaluable in the field. My 2008 Smithsonian Research Training Program intern, Ryan Stephens, measured the shrew feet. Sandra Raredon and the Division of Fishes, Department of Vertebrate Zoology, National Museum of Natural History, kindly provided access to their digital X-ray system. Roberto Portela Miguez and Paula D. Jenkins extensively searched the official registers and correspondence files at BMNH for additional information regarding their shrews from Alta Verapaz. The following curators and collection managers provided access to valuable specimens under their care: N. B. Simmons, R. S. Voss, and E. Westwig (AMNH); P.D. Jenkins, R. Portela M., and L. Tomsett (BMNH); L. R. Heaney, B. D. Patterson, and W. S. Stanley (FMNH); R. M. Timm (KU); J. M. Chupasko (MCZ); and P. Myers and S. Hinshaw (UMMZ). R. T. Chesser, S. Feinstein, A. L. Gardner, and two anonymous reviewers provided valuable comments on previous versions of this manuscript. Any use of trade, product, or firm names is for descriptive purposes only and does not imply endorsement by the U.S. government.

REFERENCES

Alston ER. 1877a. On two new species of *Hesperomys*. *Proceedings of the Zoological Society of London* **1876:** 755–757.

Alston ER. 1877b. On an undescribed shrew from Central America. *Proceedings of the Zoological Society of London* **1876:** 445–446.

Choate JR. 1970. Systematics and zoogeography of Middle American shrews of the genus *Cryptotis*. *University of Kansas Publications, Museum of Natural History* **19:** 195–317.

Fischer G. 1814. *Zoognosia tabulis synopticis illustrata. Volumen tertium. Quadrupedum reliquorum, cetorum et montrymatum descriptionem continens*. Mosquae: Nicolai Sergeidis Vsevolozsky, 3.

Goodwin GG. 1932. Three new *Reithrodontomys* and two new *Peromyscus* from Guatemala. *American Museum Novitates* **560:** 1–5.

Gray JE. 1868. Synopsis of the species of Saccomyinae, or pouched mice, in the collection of the British Museum. *Proceedings of the Zoological Society of London* **1868:** 199–206.

Holdridge LR. 1947. Determination of world plant formations from simple climatic data. *Science* **105:** 367–368.

Hutterer R. 2005. Order Soricomorpha. In: Wilson DE, Reeder DM, eds. *Mammal species of the world*, 3rd edn. Baltimore, MD: Johns Hopkins University Press, 220–311.

ICZN [International Commission on Zoological Nomenclature]. 2006. Opinion 2164 (Case 3328). *Didelphis* Linnaeus, 1758 (Mammalia, Didelphidae): gender corrected to feminine, and *Cryptotis* Pomel, 1848 (Mammalia, Soricidae): gender fixed as masculine. *Bulletin of Zoological Nomenclature* **63:** 282–283.

Jackson HHT. 1933. Five new shrews of the genus *Cryptotis* from Mexico and Guatemala. *Proceedings of the Biological Society of Washington* **46:** 79–82.

MAGA [Ministerio de Agricultura, Ganadería y Alimentación]. 2001. *Mapa de zonas de vida Holdridge. República de Guatemala*. Guatemala City: Ministerio de Agricultura, Ganadería y Alimentación. Unidad de Políticas e Información Estratégica.

Merriam CH. 1895. Revision of the shrews of the American genera Blarina and Notiosorex. *North American Fauna* **10:** 5–34.

Merriam CH. 1897a. Descriptions of two new murine opossums from Mexico. *Proceedings of the Biological Society of Washington* **11:** 43–44.

Merriam CH. 1897b. Descriptions of five new shrews from Mexico, Guatemala, and Colombia. *Proceedings of the Biological Society of Washington* **11:** 227–230.

Merriam CH. 1901a. Synopsis of the rice rats (genus *Oryzomys*) of the United States and Mexico. *Proceedings of the Washington Academy of Sciences* **3:** 273–295.

Merriam CH. 1901b. Descriptions of 23 new harvest mice (genus *Reithrodontomys*). *Proceedings of the Washington Academy of Sciences* **3:** 547–558.

Merriam CH. 1901c. Seven small mammals from Mexico, including a new genus of rodents. *Proceedings of the Washington Academy of Sciences* **3:** 559–563.

Pomel A. 1848. Etudes sur les carnassiers insectivores (Extrait). Seconde partie. – Classification des insectivores. *Archives des Sciences Physiques et Naturelles, Genève* **9:** 244–251.

Ridgway R. 1912. *Color standards and color nomenclature*. Washington, DC: Published privately by the author.

Saussure MH. 1860. Note sur quelques mammifères du Mexique. *Revue et Magasin de Zoologie* Ser. 2 **12:** 3–11, 53–57, 99–110, 241–254, 281–293, 377–383, 425–431, 479–494.

Saussure MH. 1861. Note complémentaire sur quelques mammifères du Mexique. *Revue et Magasin de Zoologie* Ser. 2 **13:** 3–5.

Tamasiunas JMD, Miranda RM, González GR, Medina JCA, García GP, González OR, Vásquez R, Herrera L, Valladares R. 2002. *Estimación de amenazas inducidas por fenómenos hidrometeorológicos en la República de Guatemala*. Guatemala City: Programa de Emergencias por Desastres Naturales, Ministerio de Agricultura, Ganadería y Alimentación and Instituto Nacional de Sismología, Vulcanología, Meteorología e Hidrología, Ministerio de Comunicaciones, Infraestructura y Vivienda.

Thomas O. 1903. On three new forms of *Peromyscus* obtained by Dr. Hans Gadow, F.R.S., and Mrs. Gadow in Mexico. *Annals and Magazine of Natural History* Ser. 7 **11:** 484–487.

Woodman N. 2010. Two new species of shrews (Soricidae) from the western highlands of Guatemala. *Journal of Mammalogy* **91:** 566–579.

Woodman N. 2011. Nomenclatural notes and identification of small-eared shrews (Mammalia: genus *Cryptotis*) from Cobán, Guatemala, in The Natural History Museum, London. *Proceedings of the Biological Society of Washington* **124:** (in press).

Woodman N, Morgan JJP. 2005. Skeletal morphology of the forefoot in shrews (Mammalia: Soricidae) of the genus *Cryptotis*, as revealed by digital x-rays. *Journal of Morphology* **266:** 60–73.

Woodman N, Péfaur J. 2008. Order Soricomorpha Gregory, 1910. In: Gardner AL, ed. *Mammals of South America, vol. 1 marsupials, xenarthrans, shrews, and bats*. Chicago, IL: University of Chicago Press, 177–187.

Woodman N, Stephens RB. 2010. At the foot of the shrew: manus morphology distinguishes closely-related *Cryptotis goodwini* and *Cryptotis griseoventris* (Mammalia, Soricidae) in Central America. *Biological Journal of the Linnean Society* **99:** 118–134.

Woodman N, Timm RM. 1992. A new species of small-eared shrew, genus *Cryptotis* (Insectivora: Soricidae), from Honduras. *Proceedings of the Biological Society of Washington* **105:** 1–12.

Woodman N, Timm RM. 1993. Intraspecific and interspecific variation in the *Cryptotis* nigrescens species complex of small-eared shrews (Insectivora: Soricidae), with the description of a new species from Colombia. *Fieldiana, Zoology, New Series* **74:** 1–30.

Woodman N, Timm RM. 1999. Geographic variation and evolutionary relationships among broad-clawed shrews of the *Cryptotis goldmani*-group (Mammalia: Insectivora: Soricidae). *Fieldiana, Zoology, New Series* **91:** 1–35.

Woodman N, Timm RM. 2000. Taxonomy and evolutionary relationships of Phillips' small-eared shrew, *Cryptotis phillipsii* (Schaldach, 1966), from Oaxaca, Mexico (Mammalia: Insectivora: Soricidae). *Proceedings of the Biological Society of Washington* **113:** 339–355.

APPENDIX

Specimens examined

Cryptotis goodwini (22). – Guatemala: Quetzaltenango: Calel, 10 200 ft (USNM 77070, 77072–77084); Volcán Santa María, 9000–11 000 ft (USNM 77086, 77087). San Marcos: Finca La Paz, 1200 m (UMMZ 103416); S slope Volcán Tajumulco, 10 000 ft (UMMZ 99541). Baja Verapaz: 5 mi N, 1 mi W El Chol, 6000 ft (KU 64611). Chimaltenango: Santa Elena, 9900–10 000 ft (FMNH 41791–41794); Tecpán, 9700 ft (AMNH 74302). Totonicapan: Cumbre María Tecún, 3000 m (UMMZ 112004–112011).

Cryptotis griseoventris (10). – Mexico: Chiapas: San Cristóbal de las Casas, 8000–9500 ft (USNM 75886–75894); 6 mi SE San Cristóbal de las Casas (MCZ 48061).

Cryptotis lacertosus (8). – Guatemala: Huehuetenango: 5 km SW San Mateo Ixtatán, 3110 m (USNM 569420, 569431, 569442, 569443, 569503); Yaiquich [*c*. 15°45′44″N, 91°30′10″W], 2680 m (USNM 569368); San Mateo Ixtatán, *c*. 4 km NW Santa Eulalia, Yaiquich, 2950 m (UMMZ 117843); 3.5 mi SW San Juan Ixcoy, 10 120 ft (KU 64610).

Cryptotis magnimanus (1). – Honduras: Comayagua: 2.5 km N, 1.6 km E Cerro San Juanillo, Reserva Biológica Cordillera de Montecillos, 1730 m (KU 144611).

Cryptotis mam (27). – Guatemala: Huehuetenango: Todos Santos Cuchumatán, 10 000 ft (USNM 77051–77064, 77066–77068); Hacienda Chancol, 9500–11 000 ft (USNM 77069); Laguna Magdalena, 2925 m (USNM 569554, 569555, 570337, 570340); Puerta del Cielo, 3350 m (USNM 570248); Aldea El Rancho, 3020 m (USNM 570256, 570257, 570313, 570314).

Cryptotis oreoryctes (7). – Guatemala: Alta Verapaz: Chelemhá, 2090 m (USNM 569854, 569877, 569878); Cobán [BMNH 7.1.1.35, 43.9.15.5, 43.10.28.7 (skull of 43.9.15.5)]; 'Verapaz' (BMNH 68.2.10.5).